Available online at www.sciencedirect.com

ScienceDirect

Mendeleev Commun., 2021, **31**, 454–455

Mendeleev Communications

Hole transporting electrodeposited PEDOT–polyelectrolyte layers for perovskite solar cells

Varvara A. Kabanova,* Oxana L. Gribkova, Alexey R. Tameev and Alexander A. Nekrasov

A. N. Frumkin Institute of Physical Chemistry and Electrochemistry, Russian Academy of Sciences, 119071 Moscow, Russian Federation. E-mail: kabanovavar@gmail.com

DOI: 10.1016/j.mencom.2021.07,005

Thin layers of poly(3,4-ethylenedioxythiophene) complexes with various sulfonated polyelectrolytes were formed electrochemically in a galvanostatic regime. These transparent hole transport layers were used in $CH_3NH_3PbI_3$ perovskite solar cells and the influence of the polyelectrolyte structure on the device performance was featured.

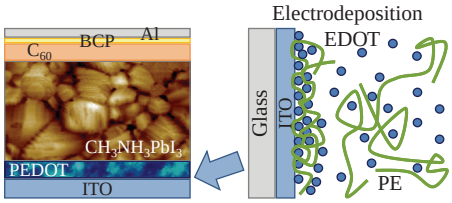

Keywords: PEDOT, electropolymerization, polyelectrolyte, perovskite, solar cell.

Perovskite solar cells (PSCs) are of current interest due to their panchromatic light absorption capacity, low rate of exciton recombination, high mobility of charge carriers, and availability of precursors for their fabrication. They can provide a power conversion efficiency (PCE) higher than 25%, as demonstrated for small area devices.[1] The scaling of solar cells makes it possible to improve the quality of interfaces between functional layers[2–5] and the intrinsic stability of perovskite materials.[6,7]

In inverted architecture PSCs, poly(3,4-ethylenedioxythiophene)–poly(styrenesulfonate) (PEDOT PSS) and nickel oxide films are frequently employed as hole transport layers (HTLs).[8–12] However, an HTL prepared from an aqueous dispersion of PEDOT–PSS obtained by the oxidative chemical polymerization of 3,4-ethylenedioxythiophene (EDOT)[13] has drawbacks such as increased acidity, which causes anode degradation with time, and hygroscopicity, which affects the HTL conductivity and the formation of a perovskite layer.[8] Electrochemical synthesis of a PEDOT layer in the presence of a polyelectrolyte makes it possible to avoid these drawbacks due to the precise control over both the morphology and thickness of layers by varying the parameters of electrosynthesis (potential, current, charge, temperature, pH, *etc.*). It affords layers without oxidant impurities and allows one to perform deposition on large areas or curved substrates, making this technology compatible with large-scale applications. Electrochemical polymerization of EDOT results in a highly conductive and transparent PEDOT film at the anode. Successful applications of electrodeposition to the preparation of PEDOT as an HTL in organic solar cells (OSCs) have been reported,[15–19] whereas this in PSCs has only been described once[14] to our best knowledge.

In this work, we electrochemically synthesized PEDOT layers on ITO in the presence of different polyelectrolytes (PEs) (see Online Supplementary Materials) and fabricated inverted PSCs based on the PEDOT–PE layers. The influence of the polyelectrolyte structure on the device performance was revealed.

The PEDOT layers electrochemically obtained in a galvanostatic mode have good homogeneity and adherence to a substrate.[19] The synthesis of PEDOT in PE-containing aqueous media proceeds at potentials ranging from 0.83 to 0.88 V (Figure S1). The synthesis potential increases in the order of decreasing hydrophobic properties of PEs (PSS > *t*-PAS ~*i*-PAS > PAMPS). In the case of the salt forms of PEs, the electrosynthesis proceeds at higher potentials than with acid forms.

Figure 1 shows the AFM images of the surfaces of electrodeposited PEDOT–PSSA and perovskite layers. The PEDOT layers have a globular structure and roughness ranging from 3.7 (PEDOT–*t*-PASA) to 14.9 nm (PEDOT–PAMPSNa), which is slightly higher than that of PEDOT–PSS(SC) (2.1 nm). The roughness of PEDOT layers obtained in the presence of the acid forms of PEs is lower than that of the layers prepared with the salt forms. The average and maximum sizes of crystals in a perovskite layer spin-coated on top of the PEDOT–PSSA layer are 200–300 and 500 nm, respectively [Figure 1(*b*)].

Optical spectra (Figure S2) of PEDOT layers are characterized by high absorption at 650 nm (polaron) extending to the NIR region, which indicates the formation of a highly conductive bipolaron form of PEDOT.[21,22] The similarity of the spectra of PEDOT layers obtained in the presence of flexible-chain PEs and a salt form of rigid-chain PEs suggests their similar doping levels. The optical absorption spectra of PEDOT complexes with rigid-chain polyacids exhibit a pronounced absorption band at 650–700 nm, which indicates the preferential formation of polarons.[21,22] In this case, the absorption band of bipolarons in the NIR region is almost absent. The PEDOT complexes with rigid-chain polyacids consist of short chains with low delocalization of charge carriers.[19]

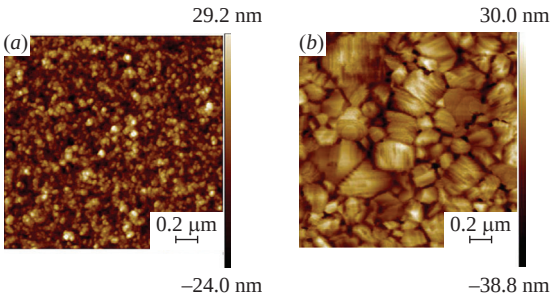

Figure 1 AFM images of (*a*) an electrodeposited PEDOT–PSSA layer and (*b*) a perovskite layer.

Table 1 Parameters of PSCs with an HTL formed from PEDOT–polyelectrolyte complexes: short-circuit current density (J_{sc}), open circuit voltage (V_{oc}), fill factor (FF), and power conversion efficiency (PCE).

HTL	J_{sc} / mA cm^{-2}	V_{oc} /V	FF (%)	PCE (%)
PEDOT–PAMPSA	17.17	0.88	69.06	10.43
PEDOT–PAMPSNa	18.99	0.79	65.19	9.78
PEDOT–PSSA	14.11	0.83	71.31	8.35
PEDOT–PSSNa	12.14	0.87	87.24	9.23
PEDOT–*i*-PASA	11.23	0.72	60.71	4.90
PEDOT–*i*-PASNa	12.39	0.83	78.93	8.13
PEDOT–*t*-PASA	12.59	0.88	56.96	6.34
PEDOT–*t*-PASNa	18.17	0.83	73.65	11.11
PEDOT : PSS(SC)	19.90	0.90	66.03	11.80

The high transmittance (60–70%) of electrodeposited PEDOT layers in the whole visible spectral range [Figure S2(*c*)] is advantageous for their use as an HTL in PSCs.

A typical current density (*J*) *versus* voltage (*V*) characteristic is presented in Figure S3 (the *J*–*V* curves were recorded for the best device based on electrodeposited PEDOT–*t*-PASA). A minor hysteresis effect can originate from the imbalance in hole and electron transport, which promotes charge accumulation either at the interface or at traps.[23] Table 1 summarizes the parameters of the PSCs for forward scans. The device performance strongly depends on the structure of PE, which promotes the deposition of PEDOT. The current density, open circuit voltage, and power conversion efficiency of the PSCs based on electrodeposited PEDOT layers are comparable with those based on spin coated PEDOT : PSS(SC) layers.

The PSCs based on the complexes of PEDOT with PAMPSA, PAMPSNa and *t*-PASNa demonstrate a maximum short-circuit current and, consequently, PCE. The degree of charge delocalization in PEDOT affects the short-circuit current: the higher the degree, the larger the short-circuit current (see Table 1). The influence of the rigidity of PE molecules is clearly revealed when the complexes of PEDOT–PAMPSNa (flexible-chain PE) and PEDOT–*t*-PASA (rigid-chain PE) are compared: the short-circuit current is larger in a device based on the former than that on the latter. These data correlate well with those obtained for polymer solar cells based on PEDOT complex as an HTL,[19] where the decreased hole transfer rate was supposed to correspond with the strong localization of radical cations on the short chains of PEDOT complexes with rigid-chain polyacids. During electrodeposition, flexible PE chains, obviously, prevent the PANI fragments from packing in the form of conductive channels to a lesser extent than rigid chains. In other words, charge percolation pathways are believed to be denser in the layer of a PEDOT complex based on flexible-chain PE than on the rigid-chain PE. Note that such conductive channels did not manifest themselves in the PANI layer casted from solution.[24]

Finally, the acid or salt forms of PEs also affect the parameters of the devices. This can originate from the dependence of HTL work-function on PE and the formation of dipoles at an interface between HTL and ITO, so revealing the electron states and work-function of the PEDOT complexes can lead to further improving the device operation.

Thus, electrodeposited thin layers of PEDOT complexes with sulfonated polyelectrolytes are applicable as a transparent hole transport layer for inverted perovskite solar cells. The parameters of devices depend on the composition of the PEDOT–polyelectrolyte complexes and the structure and form of the polyelectrolyte.

This work was supported by the Russian Foundation for Basic Research (project no. 19-29-08048_mk, PEDOT electrodeposition and project no. 18-29-23045, photovoltaic research) and the Ministry of Education and Science of the Russian Federation (providing facilities). The UV-VIS-NIR spectroscopic and AFM measurements were performed using the equipment of CKP FMI IPCE RAS.

Online Supplementary Materials

Supplementary data associated with this article can be found in the online version at doi: 10.1016/j.mencom.2021.07.005.

References

1 J. Y. Kim, J.-W. Lee, H. S. Jung, H. Shin and N.-G. Park, *Chem. Rev.*, 2020, **120**, 7867.
2 A. B. Nikolskaia, M. F. Vildanova, S. S. Kozlov and O. I. Shevaleevskiy, *Russ. Chem. Bull., Int. Ed.*, 2020, **69**, 1245 (*Izv. Akad. Nauk, Ser. Khim.*, 2020, 1245).
3 A. S. Sizov, E. V. Agina and S. A. Ponomarenko, *Russ. Chem. Rev.*, 2019, **88**, 1220.
4 O. L. Gribkova, V. A. Kabanova, A. R. Tameev and A. A. Nekrasov, *Tech. Phys. Lett.*, 2019, **45**, 858.
5 Y. B. Martynov, R. G. Nazmitdinov, A. Moià-Pol, P. P. Gladyshev, A. R. Tameev, A. V. Vannikov and M. Pudlak, *Phys. Chem. Chem. Phys.*, 2017, **19**, 19916.
6 E. I. Marchenko, S. A. Fateev, A. A. Petrov, E. A. Goodilin and A. B. Tarasov, *Mendeleev Commun.*, 2020, **30**, 279.
7 D. V. Amasev, V. G. Mikhalevich, A. R. Tameev, S. R. Saitov and A. G. Kazanskii, *Semiconductors*, 2020, **54**, 654.
8 S. Wang, T. Sakurai, W. Wen and Y. Qi, *Adv. Mater. Interfaces*, 2018, **5**, 1800260.
9 K. Sun, S. Zhang, P. Li, Y. Xia, X. Zhang, D. Du, F. H. Isikgor and J. Ouyang, *J. Mater. Sci. Mater. Electron.*, 2015, **26**, 4438.
10 I. J. Park, M. A. Park, D. H. Kim, G. Do Park, B. J. Kim, H. J. Son, M. J. Ko, D.-K. Lee, T. Park, H. Shin, N.-G. Park, H. S. Jung and J. Y. Kim, *J. Phys. Chem. C*, 2015, **119**, 27285.
11 I. J. Park, G. Kang, M. A. Park, J. S. Kim, S. W. Seo, D. H. Kim, K. Zhu, T. Park and J. Y. Kim, *ChemSusChem*, 2017, **10**, 2660.
12 D. S. Saranin, V. N. Mazov, L. O. Luchnikov, D. A. Lypenko, P. A. Gostishev, D. S. Muratov, D. A. Podgorny, D. M. Migunov, S. I. Didenko, M. N. Orlova, D. V. Kuznetsov, A. R. Tameev and A. Di Carlo, *J. Mater. Chem. C*, 2018, **6**, 6179.
13 S. Kirchmeyer and K. Reuter, *J. Mater. Chem.*, 2005, **15**, 2077.
14 R. Po, C. Carbonera, A. Bernardi and N. Camaioni, *Energy Environ. Sci.*, 2011, **4**, 285.
15 E. Nasybulin, S. Wei, I. Kymissis and K. Levon, *Electrochim. Acta*, 2012, **78**, 638.
16 Y. Vlamidis, M. Lanzi, E. Salatelli, I. Gualandi, B. Fraboni, L. Setti and D. Tonelli, *J. Solid State Electrochem.*, 2015, **19**, 1685.
17 J.-H. Huang, Z.-Y. Ho, D. Kekuda, C.-W. Chu and K.-C. Ho, *J. Phys. Chem. C*, 2008, **112**, 19125.
18 J. Yan, C. Sun, F. Tan, X. Hu, P. Chen, S. Qu, S. Zhou and J. Xu, *Sol. Energy Mater. Sol. Cells*, 2010, **94**, 390.
19 O. L. Gribkova, O. D. Iakobson, A. A. Nekrasov, V. A. Cabanova, V. A. Tverskoy, A. R. Tameev and A. V. Vannikov, *Electrochim. Acta*, 2016, **222**, 409.
20 E. A. Erazo, D. Castillo-Bendeck, P. Ortiz and M. T. Cortés, *Synth. Met.*, 2019, **257**, 116178.
21 M. Łapkowski and A. Proń, *Synth. Met.*, 2000, **110**, 79.
22 E. G. Tolstopyatova, N. A. Pogulaichenko, S. N. Eliseeva and V. V. Kondratiev, *Russ. J. Electrochem.*, 2009, **45**, 252 (*Elektrokhimiya*, 2009, **45**, 270).
23 D. H. Song, M. H. Jang, M. H. Lee, J. H. Heo, J. K. Park, S.-J. Sung, D.-H. Kim, K.-H. Hong and S. H. Im, *J. Phys. D: Appl. Phys.*, 2016, **49**, 473001.
24 O. D. Iakobson, O. L. Gribkova, A. R. Tameev, A. A. Nekrasov, D. S. Saranin and A. Di Carlo, *J. Ind. Eng. Chem.*, 2018, **65**, 309.

Received: 1st March 2021; Com. 21/6467